Advances in Nano Research, *Vol. 13, No.4 (2022) 341-350*
https://doi.org/10.12989/anr.2022.13.4.341

Continuous element method for aeroacoustics' waves in confined ducts

Mohamed A. Khadimallah*[1,2], Imene Harbaoui[3], Jean B. Casimir[5], Lamjed H. Taieb[1,4], Muzamal Hussain[6] and Abdelouahed Tounsi[7,8]

[1]*Department of Civil Engineering, College of Engineering in Al-Kharj, Prince Sattam Bin Abdulaziz University, Al-Kharj, 11942, Saudi Arabia*
[2]*Laboratory of Systems and Applied Mechanics, Polytechnic School of Tunisia, University of Carthage, Tunis, Tunisia*
[3]*Laboratory of Applied Mechanics and Engineering LR-MAI, University Tunis El Manar- -ENIT BP37- Le belvédère, 1002, Tunis*
[4]*Research Laboratory of applied fluid mechanics, process engineering and environment, National Engineering School of Sfax, Sfax University, Tunisia*
[5]*Institut Supérieur de Mécanique de Paris, Quartz (EA 7393), 3 rue Fernand Hainaut, Saint-Ouen 93407, France*
[6]*Department of Mathematics, Govt. College University Faisalabad, 38040, Faisalabad, Pakistan*
[7]*YFL (Yonsei Frontier Lab), Yonsei University, Seoul, Korea*
[8]*Department of Civil and Environmental Engineering, King Fahd University of Petroleum and Minerals, 31261 Dhahran, Eastern Province, Saudi Arabia*

(*Received November 3, 2020, Revised August 7, 2022, Accepted August 10, 2022*)

Abstract. The continuous elements method, also known as the dynamic stiffness method, is effective for solving structural dynamics problems, especially over a large frequency range. Before applying this method to fluid-structure interactions, it is advisable to check its validity for pure acoustics, without considering the different coupling parameters. This paper describes a procedure for taking wave propagation into account in the formulation of a Dynamic Stiffness Matrix. The procedure is presented in the context of the harmonic response of acoustic pressure. This development was validated by comparing the harmonic response calculations performed using the continuous element model with the analytical solution. In addition, this paper illustrates the application of this method to a simple compressible flow problem, since it has been applied solely to structural problems to date.

Keywords: acoustic; continuous element; dynamic stiffness; flow; wave propagation

1. Introduction

Acoustic flow has been the subject of much research in recent years. Hossein Kavusi and Davood Toghraie (2017) investigated a fluid flow in a heat pipe in the two dimensional state, using the finite volume numerical method based on the thermal performance of the pipe. Moraveji and Toghraie studied the effect of changing various parameters such as number of inlets, tube length, and diameter of cold outlet. Another numerical method for simulation of flow boiling was used to show the effect of increasing the velocity of a fluid jet of water on the convective heat transfer (Toghraie 2016).

The heat transfer rate as important parameter in some industrial applications was investigated to show the effect of the cavity angle and the tube size. Soroush *et al*. (2018). Laminar flow of non-Newtonian nano fluid in a two dimensional horizontal microtube with various boundary conditions was investigated to offer a good option for nano scale and microscale simulation. Rahmati *et al*. (2018).

Simon Marié *et al*., (2009), focused on the plane wave dispersion and dissipation for various kinds of discretization of the 3D linearized and isothermal Navier-Stokes equation, without taking into account stability problems. Sharma *et al*. (2020) studied the Lattice Boltzmann methods and their efficiency to solve diverse flow problems such as aero-dynamics, aeroacoustics and thermal multiphase flows. Li *et al*. (2006) used Lattice Boltzmann method to simulate fluid motions by tracking the evolution of the particle velocity distribution function based on linear streaming with non-linear collision. The accuracy of the LBM is established by comparing with direct numerical simulation (DNS) results obtained by solving the governing equations using a finite difference scheme. The proposed LBM and the DNS give identical results, thus suggesting that the LBM can be used to simulate aeroacoustics problems correctly. In the case of a uniform flow, the problem can be reduced by simple geometric transformation to a system of four standard equations of wave propagation in a medium at rest. Many studies have investigated the case of a non-uniform flow; these works have been based essentially on linearized Euler equations, Galbrun's equation, or the potential acoustic equation (Bonnet-Ben Dhia *et al*. 2001). Changes in sections of ducts generally lead to reflection phenomena that disrupt the propagation of acoustic waves (Gabard *et al*. 2004). When the section varies slowly, as in the case of turbojet aircraft, mathematical equations can be used, such as Galbrun equations (Redon 1996). In cases of sudden variation of sections, as in the mufflers generally used to reduce noise, transmission loss T_L can be simulated using finite element method [FEM] tools such as Comsol or the transfer matrix method; in both cases the flow become

*Corresponding author, Associate Professor, Ph.D.,
E-mail: am.khadimallah@gmail.com;
mohamedamine.khadimallah@fsgf.rnu.tn

ISSN: 2287-237X (Print), 2287-2388 (Online)

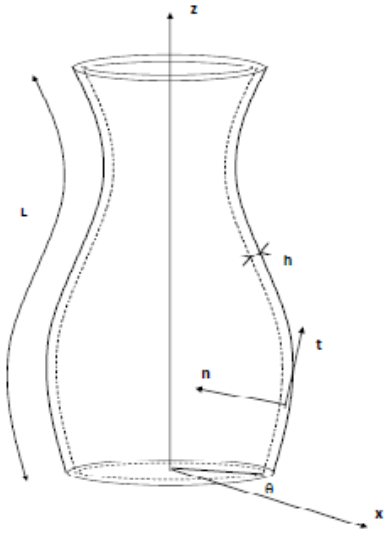

Fig. 1 Axisymmetric duct. (Batoz 1990)

quasi-one-dimensional. Magrab (1975) and Ben Tahar and Goy (1998) developed a variation formulation to study vibro-acoustic problems in the presence of a flow. They added a Lagrange multiplier to ensure the continuity of pressure at the fluid-structure interface. Ben Tahar and Dias (1999) subsequently developed a coupled FEM / BEM formulation to highlight the acoustic radiation that is conducted in the presence of a flow. The finite element model and the boundary element method are effective for low frequencies (less than 300Hz) but they do not support reliable analyses for medium frequency bands (500 Hz - 5000 Hz). This difficulty can be overcome by applying the "Dynamic Stiffness Method" for relatively simple structures: assemblies of girders, beams, plates, and revolving shells (Khadimallah *et al*. 2011). This method, which cleverly combines analytical modeling and digital assembly, reduces solution time and memory demand (Tahar and Dias 1999). Recently some researcher used different methods for nonlinear modeling (Eltaher *et al*. 2019, Ebrahimi *et al*. 2019, Safaei *et al*. 2019, Shahsavari *et al*. 2019, Benmansour *et al*. 2019).

In this study, we showed how the continuous element method (Casimir *et al*. 2007), previously used for structural dynamics, can be adapted to other kinds of problem, particularly the problem of compressible flows. We investigated the cases of a straight duct, a conical duct and an expansion chamber with and without flow, where the Mach number reached 0.3. The choice of these problems will eventually allow the method to be extended to coupled fluid flow problems and structural vibration. First, a compressible flow in an axisymmetric tube was considered. The geometry of the tube is described in Fig. 1; r is the radius of the tube, according to axis z through the center.

2. Materials and methods

Considering the density ρ of the fluid and its velocity v, the mass conservation and momentum equations for an elementary slice can be written as follows

$$\frac{\partial \rho}{\partial t}A(z)+\frac{\partial(\rho v A)}{\partial z}=0 \tag{1}$$

$$\frac{\partial \rho v}{\partial t}A(z)+v\frac{\partial \rho v}{\partial z}A(z)=\frac{\partial p}{\partial z}A(z) \tag{2}$$

where A is the duct cross section, and p is the constant pressure considered in this section for a one dimensional model. For acoustical waves, the small perturbation hypothesis gives:

$$\begin{cases} A(z)\dfrac{\partial \delta\rho}{\partial t}+\rho_0 A(z)\dfrac{\partial \delta v}{\partial z}+\rho_0\delta v\dfrac{\partial A}{\partial z}=0 \\ \rho_0\dfrac{\partial \delta v}{\partial t}=-\dfrac{\partial \delta p}{\partial z} \end{cases} \tag{3}$$

where δp, δv and $\delta\rho$ are propagating respectively small perturbations of pressure, velocity and mass density. ρ_0 is the mass density of the fluid. For isentropic transformation, $\delta\rho=\chi_s\rho_0\delta p$ where χ_s is the isentropic compressibility.

Sound wave equations in the duct become the following:

$$\begin{cases} A(z)\chi_s\dfrac{\partial \delta p}{\partial t}+A(z)\dfrac{\partial \delta v}{\partial z}+\rho_0\delta v\dfrac{\partial A}{\partial z}=0 \\ \rho_0\dfrac{\partial \delta v}{\partial t}=-\dfrac{\partial \delta p}{\partial z} \end{cases} \tag{4}$$

We seek monochromatic solutions such that $\delta p=\delta p_0(z)e^{i\omega t}$ and $\delta v=\delta v_0(z)e^{i\omega t}$, where $p_0(z)$ and $v_0(z)$ are functions of space variable z. In this case, the conservation equations are written as follows:

$$\begin{cases} i\omega\boldsymbol{\chi_s}A\delta p_0(z)+\dfrac{\partial \delta v_0}{\partial z}A+\delta v_0(z)\dfrac{\partial A}{\partial z}=0 \\ \delta v_0(z)=-\dfrac{1}{i\omega\rho_0}\dfrac{\partial \delta p_0}{\partial z} \end{cases} \tag{5}$$

and with the following matricial form:

$$\begin{pmatrix} \dfrac{\partial \delta v_0}{\partial z} \\ \dfrac{\partial \delta p_0}{\partial z} \end{pmatrix}=\begin{pmatrix} -\dfrac{1}{A}\dfrac{\partial A}{\partial z} & -i\omega\boldsymbol{\chi_s} \\ -i\omega\rho_0 & 0 \end{pmatrix}\begin{pmatrix} \delta v_0 \\ \delta p_0 \end{pmatrix} \tag{6}$$

Thus, by setting $E=(\delta v_0.\delta p_0)^T$ and $D(z.\omega)=\begin{pmatrix} -\frac{1}{A}\frac{\partial A}{\partial z} & -i\omega\chi_s \\ -i\omega\rho_0 & 0 \end{pmatrix}$. Eq. (6) takes the form:

$$\frac{dE}{dz}=[D(z.\omega)]E(z) \tag{7}$$

3. Continuous element method

Considering position z along the z, we can define a matrix $T_\omega(z)$ called the Dynamic Transfer Matrix,

$$E_\omega(z)=T_\omega(z)E_\omega(0) \tag{8}$$

The matrix, $T_\omega(0)$, satisfies:

$$E_\omega(0)=T_\omega(0)E_\omega(0) \tag{9}$$

and therefore,

$$\frac{dT_\omega(z)}{dz}=[D_\omega(z)]T_\omega(z) \tag{10}$$

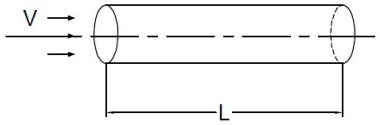

Fig. 2 Straight duct with uniform flow

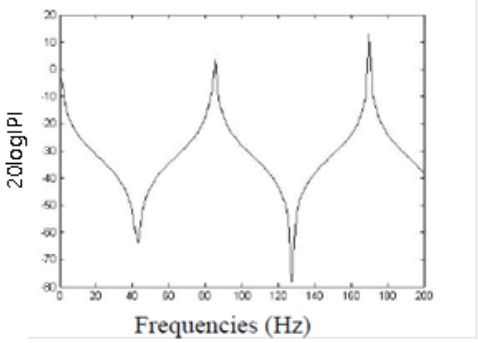

Fig. 3 Pressure response in the case of a fluid propagation without flow

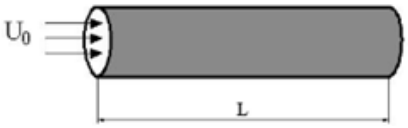

Fig. 4 Straight duct with uniform flow

Thus the dynamic transfer matrix $T_\omega(z)$ satisfies the linear differential equation of the first order parameterized by ω and defined by the differential dynamic matrix $D_\omega(z)$. The solution of this first-order equation is obtained by introducing the concept of the exponential matrix. The dynamic transfer matrix can be written as follows:

$$[T_\omega(z)] = e^{\int_0^z D_\omega(l)dl} \tag{11}$$

Function $e^{[X]}$, defined on the set of matrices of dimension n is defined by

$$e^{[X]} = \sum_{i=0}^{\infty} \frac{[X]^i}{i!} \tag{12}$$

3.1 Acoustical spectral elements with internal flow

3.1.1 Straight ducts

We now consider a uniform flow with constant velocity V in a duct subjected to harmonic excitation. The medium is considered homogeneous and non-dissipative (see Fig. 2).

L = 2 m, c_0 = 340 m/s, ρ_0 = 1.2 Kg/m^3, S = 0.78m^2, P_0 = 10 N/m^2.

First, we consider a fluid in a cylindrical duct without introducing flow parameters; thus, we can write the following:

$$\begin{pmatrix} \frac{\partial \delta v_0}{\partial z} \\ \frac{\partial \delta p_0}{\partial z} \end{pmatrix} = \begin{pmatrix} 0 & -i\omega\chi_s \\ -i\omega\rho_0 & 0 \end{pmatrix} \begin{pmatrix} \delta v_0 \\ \delta p_0 \end{pmatrix} \tag{13}$$

Finally, matrix $[T(\omega)]$ is written as follows:

$$[T_\omega(z)] = e^{\int_0^z D_\omega(l)dl} \tag{14}$$

Thus, using the dynamic stiffness matrix [K], equation (13) can be written as follows:

$$\begin{pmatrix} \delta p_0(0) \\ \delta p_0(L) \end{pmatrix} = [K(\omega)] \begin{pmatrix} \delta v_0(0) \\ \delta v_0(L) \end{pmatrix} \tag{15}$$

$$[K(\omega)] = \frac{1}{i\rho_0 c} \begin{pmatrix} cotg\frac{\omega}{c}L & -\frac{1}{\sin\frac{\omega}{c}\,\mathrm{L}} \\ \frac{1}{\sin\frac{\omega}{c}\,\mathrm{L}} & -cotg\frac{\omega}{c}L \end{pmatrix} \tag{16}$$

From this expression, we obtain the response in terms of pressure as shown in Fig. 3 which describes a propagation wave in a tube without flow. We now consider a uniform flow (Fig. 4) with constant velocity U_0 in a duct subject to harmonic excitation at a point on its surface. The medium is considered homogeneous and non-dissipative.

By introducing the wave number and the Mach number defined respectively by $k = \frac{\omega}{c}$, and $M = \frac{u_0}{c}$, we can write

$$\begin{cases} \rho_0\chi_s\frac{\partial \delta p}{\partial t} + \rho_0\frac{\partial \delta v}{\partial z} + u_0\rho_0\chi_s\frac{\partial \delta p}{\partial z} = 0 \\ \rho_0\frac{\partial \delta v}{\partial t} + u_0\rho_0\chi_s\frac{\partial \delta p}{\partial t} + 2\rho_0 u_0\frac{\partial \delta v}{\partial z} + {u_0}^2\rho_0\chi_s\frac{\partial \delta p}{\partial z} = -\frac{\partial \delta p}{\partial z} \end{cases} \tag{17}$$

We obtain the differential relation

$$\begin{cases} i\frac{k}{c}\delta p_0 + \rho_0\frac{\partial \delta v_0}{\partial z} + \frac{M}{C}\frac{\partial \delta p_0}{\partial z} = 0 \\ i\omega\rho_0\delta v_0 + ikM\delta p_0 + 2\rho_0 u_0\frac{\partial \delta v_0}{\partial z} + (1+M^2)\frac{\partial \delta p_0}{\partial z} = 0 \end{cases} \tag{18}$$

and then,

$$\begin{cases} \frac{\partial \delta v_0}{\partial z} = \frac{iMk}{1-M^2}\delta v_0 - \frac{ik}{\rho_0 c(1-M^2)}\delta p_0 \\ \frac{\partial \delta p_0}{\partial z} = \frac{iMk}{1-M^2}\delta p_0 - \frac{ik\rho_0 c}{(1-M^2)}\delta v_0 \end{cases} \tag{19}$$

with $\mathrm{k_r} = \frac{\mathrm{k}}{1-\mathrm{M}^2}$, we obtain

$$\begin{pmatrix} \frac{\partial \delta v_0}{\partial z} \\ \frac{\partial \delta p_0}{\partial z} \end{pmatrix} = \begin{pmatrix} iMk_r & -\frac{ik_r}{\rho_0 c} \\ -ik_r\rho_0 c & iMk_r \end{pmatrix} \begin{pmatrix} \delta v_0 \\ \delta p_0 \end{pmatrix} \tag{20}$$

The dynamic transfer relationship is established numerically by the approach presented in (3), with

$$[T(\omega)] = e^{iMk_rL} \begin{pmatrix} cosk_r l & -i\frac{sink_r l}{\rho_0 c} \\ -\rho_0 c\sin k_r\, l & cosk_r l \end{pmatrix} \tag{21}$$

The dynamic stiffness matrix is:

$$[K] = \begin{pmatrix} icotgk_r l & \frac{ie^{-iMk_rL}}{sink_r l} \\ e^{iMk_rL}(-\rho_0 c\sin k_r\, l + icotgk_r l\cos k_r l) & icotgk_r l \end{pmatrix} \tag{22}$$

According to Tsuji *et al.* (2002), the expressions of displacement and pressure are determined analytically by

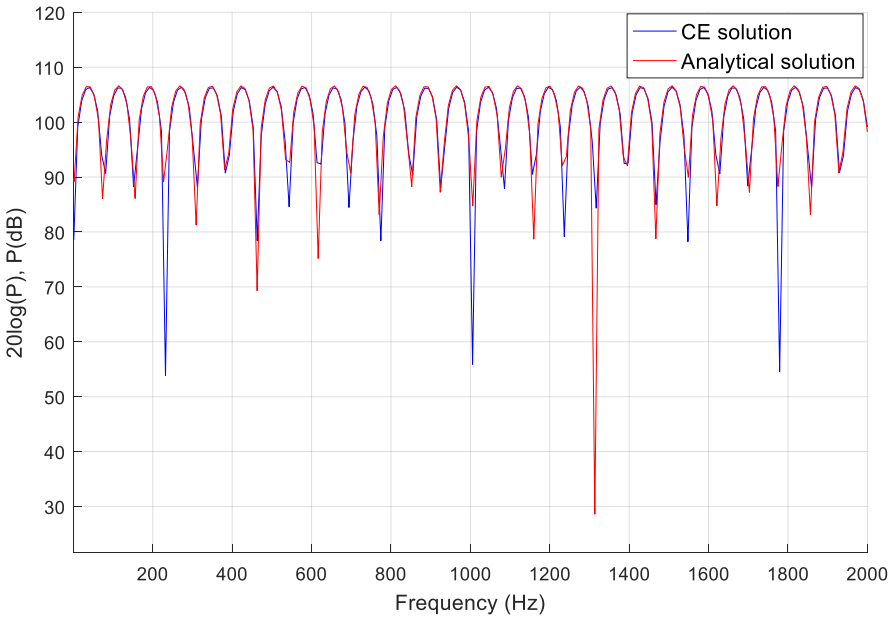

Fig. 5 FE/ CE pressure responses

solving the wave equation and are given by the following

$$U(z) = ik\left(\frac{C_1}{1+M_z}e^{-\frac{ikz}{1+M_z}} - \frac{C_2}{1-M_z}e^{\frac{ikz}{1-M_z}}\right) \quad (23)$$

$$P(z) = i\omega\rho_0\left(\frac{C_1}{1+M_z}e^{-\frac{ikz}{1+M_z}} - \frac{C_2}{1-M_z}e^{\frac{ikz}{1-M_z}}\right) \quad (24)$$

where C_1 and C_2 are constants determined from boundary conditions.

$$\begin{aligned} &\frac{\partial\emptyset}{\partial n} = -\frac{\partial\emptyset}{\partial z} = U_0 \ \ (z=0) \\ &\frac{\partial\emptyset}{\partial n} = \frac{\partial\emptyset}{\partial z} = -jk\frac{1}{\beta_T + M_z}\emptyset \quad (z=L) \\ &\frac{\partial\emptyset}{\partial n} = 0 \ \ (wall\ boundary) \end{aligned} \quad (25)$$

The particle velocity u and the sound pressure p can be expressed in terms of the velocity potential, as: $u = -\nabla\emptyset$. $p = \rho_0(\frac{\partial\emptyset}{\partial t} + v_0\nabla\emptyset)$, where $\partial/\partial n$ is the normal derivative to the boundary and $\beta_T = Z_T/\rho_0 c_0$ is the termination impedance normalized with respect to the characteristic impedance of the medium.

Using the following parameters: L=2 m, S = 0.78 m², M=0.3, P_0=10 N/m² , $\rho_0 = 1.2\ \mathrm{kg/m^3}$, $c_0 = 340\ \mathrm{m/s}$ and $u_0 = 10\ \mathrm{m/s}$, the responses in terms of pressure were obtained and then compared with those determined analytically. Fig. 5 shows the agreement between the response curves. The maximum peak error did not exceed 2% for most frequencies. The discrepancies were due to numerical errors of calculation.

3.1.2 Conical duct

We now consider a uniform flow with constant velocity v_0 in a conical duct subjected to harmonic excitation at a point on its surface. The medium is considered homogeneous and non-dissipative. The mass conservation and momentum equations are

$$\frac{\partial\rho}{\partial t}A(z) + \frac{\partial(\rho v A)}{\partial z} = 0 \quad (26)$$

$$\frac{\partial\rho v}{\partial t}A(z) + v\frac{\partial\rho v}{\partial z}A(z) = -\frac{\partial p}{\partial z}A(z) \quad (27)$$

For a steady incompressible flow, these equations are reduced to:

$$\frac{\partial\rho}{\partial t}A(z) + \frac{\partial(\rho v A)}{\partial z} = 0 \quad (28)$$

$$\frac{\partial\rho v}{\partial t}A(z) + v\frac{\partial\rho v}{\partial z}A(z) = -\frac{\partial p}{\partial z}A(z) \quad (29)$$

By applying small perturbations in Eqs. (28) and (29)

$$\begin{cases} \rho = \rho_0 + \delta\rho \\ p = p_0 + \delta p \\ v = v_0 + \delta v \end{cases} \quad (30)$$

and then subtracting the steady state Eqs. (3a) and (3b), respectively, from these equations, we obtain

$$\frac{d\rho}{dt} + \rho_0\frac{\partial\delta v}{\partial z} + \frac{\delta v\rho_0}{A(z)}\frac{dA(z)}{dz} = 0 \quad (31)$$

$$\rho_0\frac{d\delta v}{dt} + \delta v\rho_0\frac{d\delta v}{dz} = -\frac{\partial p_0}{\partial z} \quad (32)$$

We consider a conical duct of diameter D and length L with $L = z_2 - z_1$, as shown in Fig. 6.

By introducing the wave number and the Mach number, we can write

By introducing the wave number and the Mach number, we can write

$$\begin{cases} \rho_0\boldsymbol{\chi_s}\frac{\partial\delta p}{\partial t} + \rho_0\frac{\partial\delta v}{\partial z} + v_0\rho_0\boldsymbol{\chi_s}\frac{\partial\delta p}{\partial z} + \frac{v_0\rho_0}{A(z)}\frac{dA(z)}{dz} = 0 \\ \rho_0\frac{\partial\delta v}{\partial t} + v_0\rho_0\boldsymbol{\chi_s}\frac{\partial\delta p}{\partial t} + 2\rho_0 v_0\frac{\partial\delta v}{\partial z} + {v_0}^2\rho_0\boldsymbol{\chi_s}\frac{\partial\delta p}{\partial z} = -\frac{\partial\delta p}{\partial z} \end{cases} \quad (33)$$

We then obtain the differential relation as follows:

$$\begin{cases} i\dfrac{k}{c}\delta p_0 + \rho_0\dfrac{\partial \delta v_0}{\partial z} + \dfrac{M}{C}\dfrac{\partial \delta p_0}{\partial z} + \dfrac{v_0\rho_0}{A(z)}\dfrac{dA(z)}{dz} = 0 \\ i\omega\rho_0\delta v_0 + ikM(z)\delta p_0 + 2\rho_0 u_0\dfrac{\partial \delta v_0}{\partial z} \\ +(1+M(z)^2)\dfrac{\partial \delta p_0}{\partial z} = 0 \end{cases} \quad (34)$$

Using $k_r = \frac{k}{1-M^2}$

$$\begin{cases} \dfrac{\partial \delta v_0}{\partial z} = \dfrac{iM(z)k}{1-M(z)^2}\delta v_0 - \dfrac{ik}{\rho_0 c(1-M(z)^2)}\delta p_0 \\ -\dfrac{v_0}{A(z)(1-M(z)^2)}\dfrac{dA(z)}{dz} \\ \dfrac{\partial \delta p_0}{\partial z} = \dfrac{iM(z)k}{1-M(z)^2}\delta p_0 - \dfrac{ik\rho_0 c}{(1-M(z)^2)}\delta v_0 \\ +2\dfrac{{v_0}^2\rho_0}{A(z)(1-M(z)^4)}\dfrac{dA(z)}{dz} \end{cases} \quad (35)$$

In this case, M(z) is inversely proportional to A(z):

$$M(z) = M_1\left[\frac{z_1}{z}\right]^2 \quad (36)$$

Finally, matrix $[T(\omega)]$ is written as follows:

$$\begin{pmatrix} \delta v_0(L) \\ \delta p_0(L) \end{pmatrix} = e^{ikM(z)L}\begin{bmatrix} T_{11} & T_{12} \\ T_{21} & T_{22} \end{bmatrix}\begin{pmatrix} \delta v_0(0) \\ \delta p_0(0) \end{pmatrix} \quad (37)$$

where

$$T_{11} = \begin{bmatrix} \left(\dfrac{z_2}{z_1} + i\dfrac{M_1 L}{kz_1^2}\right)\cos kL + \\ \left(-\dfrac{1}{k_0 z_1} - i\dfrac{z_2}{z_1}(M_1 - M_2) - i\dfrac{M_1}{(kz_1)^2}\right)\sin kL \end{bmatrix}$$

$$T_{12} = -\frac{A_1}{c}\begin{bmatrix} i\left(\dfrac{z_2}{z_1} + \dfrac{1}{k^2 z_1^2} - iM_1\left(\dfrac{1}{kz_1} + \dfrac{1}{kz_2}\right)\right)\sin kL \\ -\left(i\dfrac{1}{kz_1^2} + \dfrac{z_2}{z_1}(M_1 - M_2)\right)\cos kL \end{bmatrix}$$

$$T_{21} = -\frac{c}{A_1}\begin{bmatrix} -\dfrac{z_1}{z_2}(M_1 - M_2)\cos kL + \\ i\left(\dfrac{z_1}{z_2} + i\dfrac{M_1}{(kz_2)^2}\left(\dfrac{z_1}{z_2}\right)^3 + 1\right)\sin kL \end{bmatrix} \quad (38)$$

$$T_{22} = \begin{bmatrix} \left(\dfrac{z_1}{z_2} - i\dfrac{M_2 L}{kz_2^2}\right)\cos kL + \\ \left(\dfrac{1}{kz_2} + i\dfrac{M_2}{k^2 z_2^2} - i\dfrac{z_1}{z_2}(M_1 - M_2)\right)\sin kL \end{bmatrix}$$

The expressions of displacement and pressure are determined analytically by solving the wave equation and are given by the following:

$$u(z,t) = e^{i\omega t}(\rho S_1 / z_1^2)e^{-ikM(z)z} \begin{bmatrix} A\{1 + jk(1-M(z))z\}e^{-ikz} \\ +B\{1 - ik(1+M(z))z\}e^{-ikz} \end{bmatrix} \quad (39a)$$

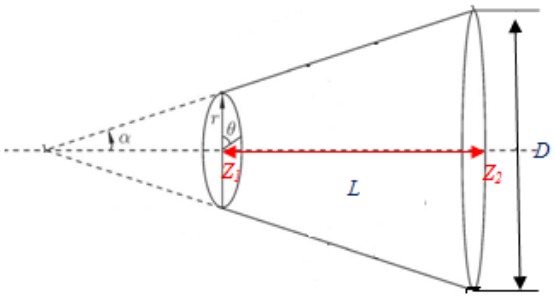

Fig. 6. Conical duct

$$p(z,t) = (\rho c_0 / z^2)e^{i\omega t}e^{-ikM(z)z} \begin{bmatrix} A\{ikz(1-M(z)) - M(z)\}e^{-ikz} \\ +B\{ikz(1+M(z)) - M(z)\}e^{-ikz} \end{bmatrix} \quad (39b)$$

with A and B being constants determined from boundary conditions.

The responses in terms of pressure were obtained and then compared with those determined analytically. Figure 7 shows agreement between the response curves. The maximum peak error did not exceed 3% for most of the frequencies.

Fig. 8 illustrates the evolution of the response spectrum in its convergence to that without flow. z_1=0.0715 m, z_2=0.4245 m, d=0.0246 m, M=0.2, P_0=1 N/m², ρ_0 = 1.2Kg/m³, c_0 = 340 m/s and u_0 = 1 m/s. A comparison between Figs. (7) and (8), indicates that in the absence of mean flow the responses obtained in terms of pressure in conical duct showed a stable behavior.

The mean flow can change these responses. Thus, the combined effects of the area change and the increase in the mean flow raises the peaks essentially in low frequency.

The pressure behavior of acoustic wave propagation reveals that it is insensitive to area changes at higher frequencies, and it passes through the duct as he would do in a straight one.

3.1.3 Continuous element for a Muffler

We now consider the propagation of an acoustic wave in a muffler or an expansion chamber. The muffler is defined as a non-uniform duct formed by multiple segments of straight uniform duct, as shown in Fig. 9. This configuration can be found in many industrial sectors. It is used to reduce the noise level of internal combustion engine exhausts, compressors, etc.

The design of the muffler consists of an enclosure of variable geometry; the parameter most commonly used to evaluate the sound radiation characteristics is transmission loss T_L. The latter is used to evaluate the acoustic performance of the muffler. The T_L is the difference in the sound power level between the incident wave entering the muffler and the transmitted wave exiting it. Beranet and Ver (1992).

$$PT_L = 10\log\frac{W_i}{W_t} \quad (40)$$

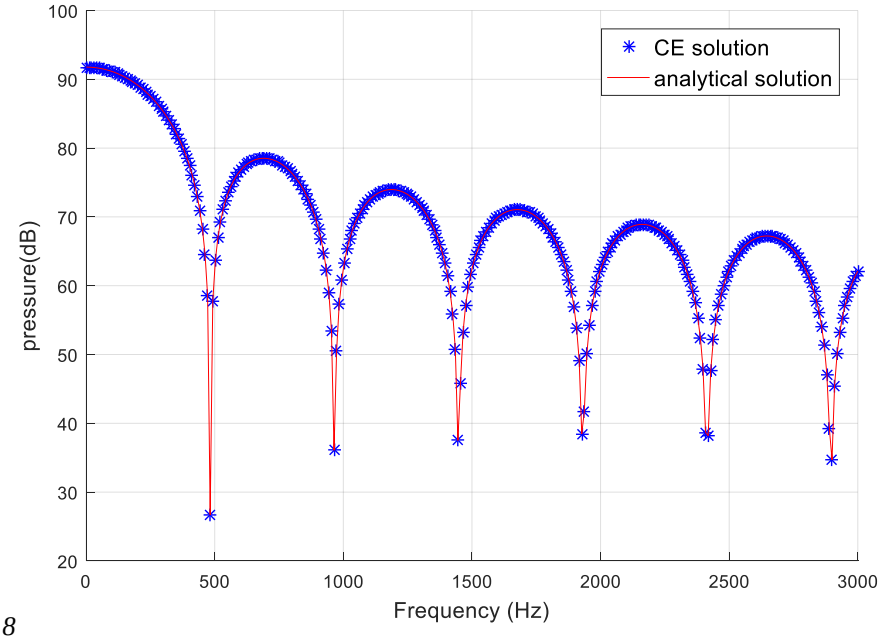

8

Fig. 7 Pressure response in a conical duct

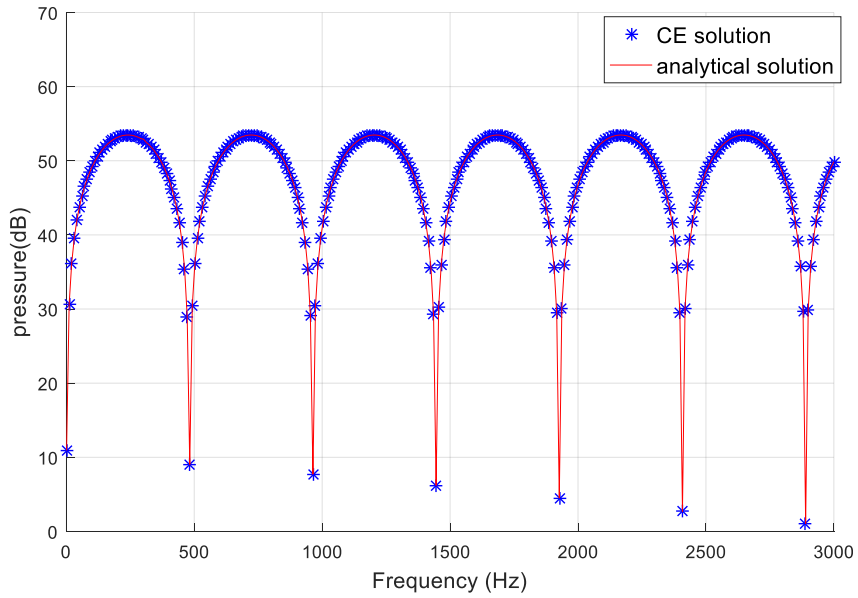

Fig. 8 Pressure response in a conical duct in the case of fluid propagation without flow

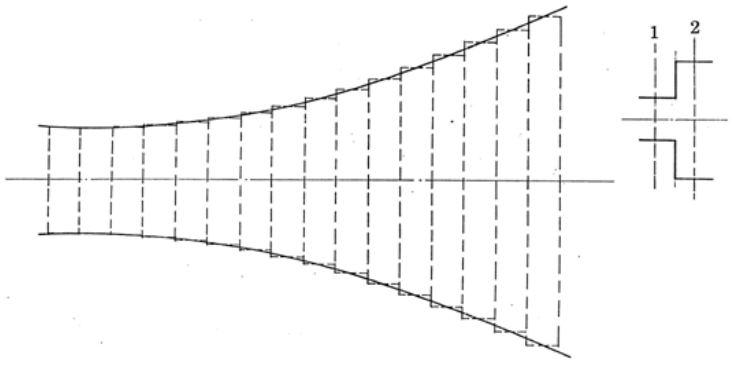

Fig. 9 Discontinuity in a duct

$W_i = \frac{{p_i}^2}{\rho_c} S_i$ is the incident sound power

$W_t = \frac{{p_t}^2}{\rho_c} S_o$ is the transmitted sound power

S_i and S_o Are muffler inlet and outlet tube sections, Therefore,

$$T_L = 20 \log \frac{p_i}{p_o} + 10 \log \frac{S_i}{S_o} \tag{41}$$

We tried to solve the acoustic problem to compute the transmission loss T_L for the muffler using the continuous element method and we validated our solution with the analytical solution. We considered a muffler with three straight ducts assuming a one dimensional propagation plane wave across each discontinuity, as shown in Figure 10. (the previous method was used to take into account the discontinuity of the considered structure).

We then defined three zones as 1, 2, and 3, with sections a-a', b-b', and c-c', respectively. For each section, we defined the transfer matrix, formulated previously in Section 3.2.

$$\begin{pmatrix} \delta v_0(a') \\ \delta p_0(a') \end{pmatrix} = Taa \begin{pmatrix} \delta v_0(a) \\ \delta p_0(a) \end{pmatrix}$$

$$\begin{pmatrix} \delta v_0(a') \\ \delta p_0(a') \end{pmatrix} = e^{iMK_r Laa'} \begin{pmatrix} \cos KL_{aa'} & -i\frac{\sin KL_{aa'}}{\rho_0 c} \\ -i\rho_0 c \sin KL_{aa'} & \cos KL_{aa'} \end{pmatrix} \begin{pmatrix} \delta v_0(a) \\ \delta p_0(a) \end{pmatrix} \tag{42}$$

$$\begin{pmatrix} \delta v_0(b') \\ \delta p_0(b') \end{pmatrix} = Tbb \begin{pmatrix} \delta v_0(b) \\ \delta p_0(b) \end{pmatrix}$$

$$\begin{pmatrix} \delta v_0(b') \\ \delta p_0(b') \end{pmatrix} = e^{iMK_r Lbb'} \begin{pmatrix} \cos KL_{bb'} & -i\frac{\sin KL_{bb'}}{\rho_0 c} \\ -i\rho_0 c \sin KL_{bb'} & \cos KL_{bb'} \end{pmatrix} \begin{pmatrix} \delta v_0(b) \\ \delta p_0(b) \end{pmatrix} \tag{43}$$

$$\begin{pmatrix} \delta v_0(c') \\ \delta p_0(c') \end{pmatrix} = Tcc \begin{pmatrix} \delta v_0(c) \\ \delta p_0(c) \end{pmatrix}$$

$$\begin{pmatrix} \delta v_0(c') \\ \delta p_0(c') \end{pmatrix} = e^{iMK_r Lcc'} \begin{pmatrix} \cos KL_{cc'} & -i\frac{\sin KL_{cc'}}{\rho_0 c} \\ -i\rho_0 c \sin KL_{cc'} & \cos KL_{cc'} \end{pmatrix} \begin{pmatrix} \delta v_0(c) \\ \delta p_0(c) \end{pmatrix} \tag{44}$$

We had two discontinuous sections; the first was the expansion section S_b and the second was the contraction section S_a. For these two sections, we defined two transfer matrices T_{ab} and T_{bc}, respectively.

$$T_{ab} = \begin{bmatrix} \frac{S_b}{S_a} & 0 \\ 0 & 1 \end{bmatrix} \tag{45}$$

and

$$T_{bc} = \begin{bmatrix} \frac{S_c}{S_b} & 0 \\ 0 & 1 \end{bmatrix} \tag{46}$$

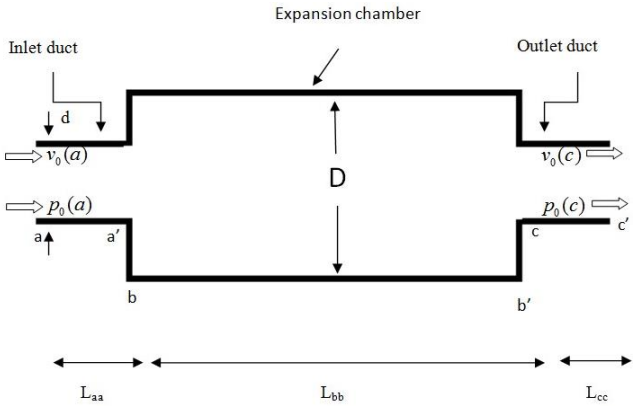

Fig. 10 Expansion chamber

then

$$\begin{pmatrix} v_0(a) \\ p_0(a) \end{pmatrix} = T(\omega) \begin{pmatrix} v_0(c) \\ p_0(c) \end{pmatrix} = T_{aa} T_{ab} T_{bb} T_{bc} T_{cc} \begin{pmatrix} v_0(c) \\ p_0(c) \end{pmatrix} \tag{47}$$

The general transfer matrix takes the following form:

$$T(w) = \begin{bmatrix} T_{11} & T_{12} \\ T_{21} & T_{22} \end{bmatrix} \tag{48}$$

The transmission loss T_L is

$$T_L = 10 \log \left[1 + \frac{1}{4} \left(m - \frac{1}{m} \right)^2 sin^2(K_r L_{bb'}) \right] \tag{49}$$

where $m = \frac{S_b}{S_a}$ and $S_a = S_c$.

For an expansion chamber with these dimensions L_{aa}, L_{bb}, and L_{cc}, which are the respective lengths of the three zones, L_{bb} represents the length of the expansion chamber equal to 0.54 m; $L_{aa} = L_{cc} = 0.10$ m; R_a, R_b, and R_c are the radii of the three zones, $R_a = R_c = 0.024295$ m and $R_b = 0.07659$ m, respectively; and S_b and S_a are the expansion section and the contraction section, respectively; $m = \frac{S_b}{S_a} = 9.938$, Mach number M=0.3, $\rho_0 = 1.2\ \mathrm{kg/m^3}$, $c_0 = 340\ \mathrm{m/s}$ and $u_0 = 1\ \mathrm{m/s}$, P_0=100 Pa.

The responses obtained using the continuous element method in terms of pressure and transmission loss were compared with those obtained analytically. The results showed agreement between the analytical solution and the continuous element solution (see Fig. 11)

Now, assuming there was no flow (M=0) in the muffler, the continuous elements were validated by comparing the transmission loss computed from the analytical solution with published experimental measurements. (Selamet *et al.* 1997).

Fig. 12 shows comparisons between the transmission loss derived from the continuous element method, the analytical solution, and the measured data. The transmission loss derived from the continuous element method matched well with the published experimental measurements over the entire frequency range. The small deviation may be due to leakage of sound, irregularity of impedance duct, and problems in producing pure white noise in experimental setup. At higher frequencies, noticeable magnitude differences are perceived. These differences are due to the

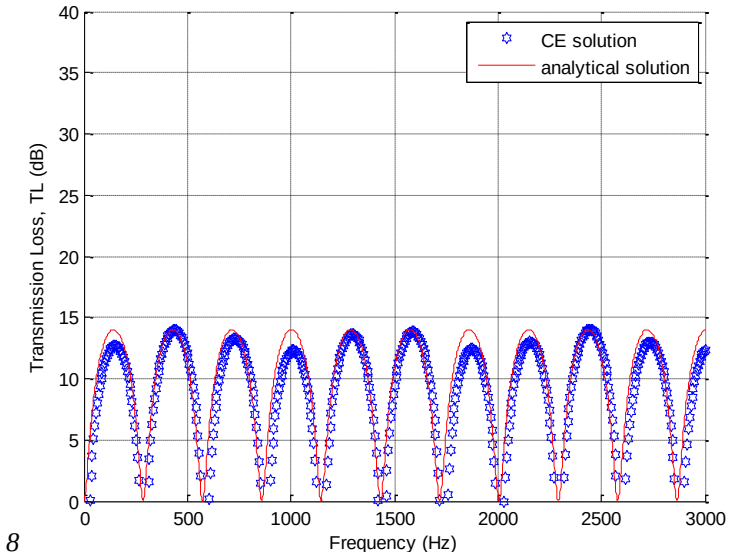

8

Fig. 11 Analytical/CE pressure responses

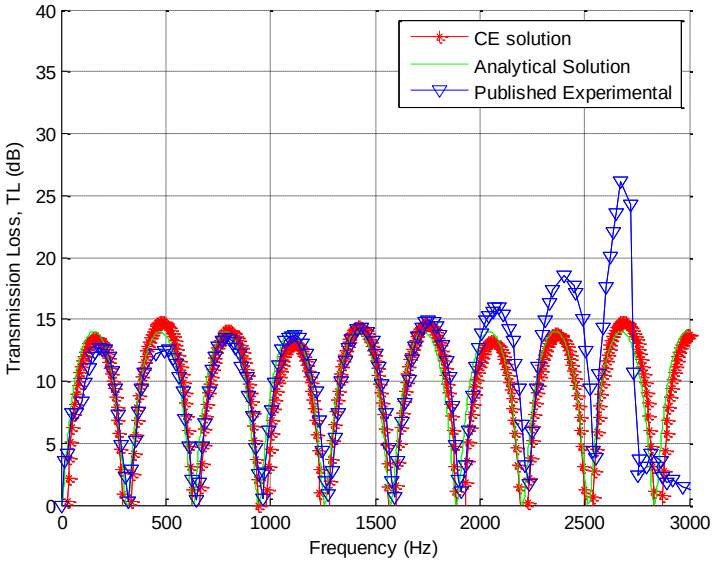

Fig. 12 T_L Comparison with EC, analytical and published experimental results. (Selamet *et al*. 1997)

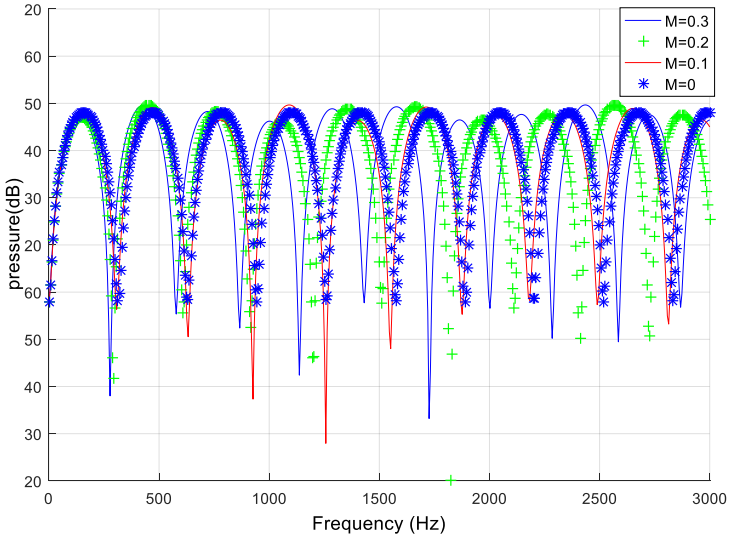

Fig. 13. Responses to different Mach numbers

fact that some Multi-dimensional waves are excited, non-planar contours begin to appear at the discontinuities area, due to the fact that the transition excites higher order radial modes with larger frequencies.

Fig. 13 illustrates the evolution of the response spectrum in a muffler in its convergence without mean flow (M=0) and with mean flow, for various Mach numbers, (M=0.3, M=0.2, and M=0.1). The differences are small, at (0-900 Hz) frequency range and became more important for higher frequencies.

4. Conclusions

The continuous element method was applied to solve the problem of propagation of an acoustic wave in a straight duct with and without flow and in a muffler composed of three straight ducts with flow. This development allowed the effectiveness of the continuous element model to be assessed, first for acoustic problems, and then for interaction with a fluid structure. The proposed method was validated by comparing the response obtained by the continuous element method in terms of pressure and transmission loss with that obtained analytically.

The advantages of the dynamic stiffness formulation in terms of accuracy, storage requirements and time consumption were preserved. Very good convergence of the FE results with the computed solution were observed for various cases. These comparisons allowed validating the procedure described. Therefore, the Continuous Elements Method offers a benchmark solution for FEM, particularly in the aeroacoustics problems. Fluid/composite interaction problems that involve distributed loads will be another field of investigation for the dynamic stiffness method.

This study can be extended by using the continuous element method with different coupling parameters in order to formulate the problem of fluid-structure interactions.

References

Moraveji, A. and Toghraie, D. (2017), "Computational fluid dynamics simulation of heat transfer and fluid flow characteristics in a vortex tube by considering the various parameters", *Int. J. Heat Mass Transf.*, **113**, 432-443. http://doi.org/10.1016/j.ijheatmasstransfer.2017.05.095.

Rahmati, A.R., Akbari, O.A., Marzban, A., Toghraie, D., Karimi, R. and Pourfattah, F. (2018), "Simultaneous investigations the effects of non-Newtonian nanofluid flow in different volume fractions of solid nanoparticles with slip and no-slip boundary conditions", *Therm. Sci. Eng. Prog.*, **5**, 263-277. https://doi.org/10.1016/j.tsep.2017.12.006.

Batoz. J.L. and Dhatt. G. (2002), "Modélisation des structures par éléments finis", *Paris: Hermes*, **3**.

Ben Tahar. M. and Goy. E., (1998), "Resolution of a vibro acoustic problem in the presence of a nonuniform mean flow", *Proceedings of the Forth AIAA Joint Aeroacoustics Conference*, Toulouse, France, June.

Benmansour, D.L., Kaci, A., Bousahla, A.A., Heireche, H., Tounsi, A., Alwabli, A.S., Alhebshi, A.M., Al-ghmady, K. and Mahmoud, S.R. (2019), "The nano scale bending and dynamic properties of isolated protein microtubules based on modified strain gradient theory", *Adv. Nano Res.*, **7**(6), 443-457. https://doi.org/10.12989/anr.2019.7.6.443.

Beranet, L.L. and Vér, I.L. (1992), *Noise and Vibration Control Engineering*', John Wiley & Sons, Inc., 374. https://doi.org/10.1002/9780470172568.

Bonnet-Ben Dhia. A.S., Legendre. G. and Lunéville E. (2001), "Mathematical analysis of Galbrun's equation with uniform flow", *Comptes Rendus de l'Académie des Sciences, Mechanics*, **329**(8), 601-606. https://doi.org/10.1016/S1620-7742(01)01373-3.

Casimir. J. B., Nguyen. M.C. and Tawfiq. I. (2007), "Thick shells of revolution: Derivation of the dynamic stiffness matrix of continuous elements and application to a tested cylinder", *Comput. Struct.*, **85**(23-24), 1845-1857. https://doi.org/10.1016/j.compstruc.2007.03.002.

Dabiri, S., Khodabandeh, E., Poorfar, A.K., Mashayekhi, R., Toghraie, D. and Zade, S.A.A. (2018), "Parametric investigation of thermal characteristic in trapezoidal cavity receiver for a linear Fresnel solar collector concentrator", *Energy*, **153**, 17-26. https://doi.org/10.1016/j.energy.2018.04.025.

Ebrahimi, F., Dabbagh, A., Rabczuk, T. and Tornabene, F. (2019). "Analysis of propagation characteristics of elastic waves in heterogeneous nanobeams employing a new two-step porosity-dependent homogenization scheme", *Adv. Nano Res.*, **7**(2), 135-143. https://doi.org/10.12989/anr.2019.7.2.135.

Eltaher, M.A., Almalki, T.A., Ahmed, K.I. and Almitani, K.H. (2019), "Characterization and behaviors of single walled carbon nanotube by equivalent-continuum mechanics approach", *Adv. Nano Res.*, **7**(1), 39-49. https://doi.org/10.12989/anr.2019.7.1.039.

Gabard. G., Treyssede. F. and Ben Taher. M. (2004), "A numerical method for vibro-acoustic problems with sheared mean flows", *J. Sound Vib.*, **272**(991), 1011. https://doi.org/10.1016/j.jsv.2003.03.007.

Kavusi, H. and Toghraie, D. (2017), "A comprehensive study of the performance of a heat pipe by using of various nanofluids", *Adv. Powder Technol.*, **28**(11), 3074-3084. https://doi.org/10.1016/j.apt.2017.09.022.

Kar, V.R., Panda, S.K., and Pandey, H.K. (2018), "Numerical study of temperature dependent eigenfrequency responses of tilted functionally graded shallow shell structures", *Struct. Eng. Mech.*, **68**(5), 527-536. https://doi.org/10.12989/sem.2018.68.5.527.

Khadimallah. M.A., Casimir. J.B., Chafra, M. and Smaoui, H., (2011), "Dynamic stiffness matrix of an axisymmetric shell and response to harmonic distributed loads", *Comput. Struct.*, **89**(5-6), 467-475. https://doi.org/10.1016/j.compstruc.2010.11.017.

Kocal, T., and Akbarov, S.D. (2019), "The influence of the rheological parameters on the dispersion of the flexural waves in a viscoelastic bi-layered hollow cylinder", *Struct. Eng. Mech.*, **71**(5), 577-601. https://doi.org/10.12989/sem.2019.71.5.577.

Li, X.M., Leung, R.C.K. and So, R.M.C. (2006), "One-step aeroacoustics simulation using lattice Boltzmann method", *AIAA J.*, **44**(1), 78-89.

Magrab. E.B. (1975), *Environmental Noise Control*, John Wiley & Sons, New York, U.S.A.

Marié, S., Ricot, D. and Sagaut, P. (2009), "Comparison between lattice Boltzmann method and Navier-Stokes high order schemes for computational aeroacoustics, *J. Comput. Phys.*, **228**, 1056-1070. https://doi.org/10.1016/j.jcp.2008.10.021.

Redon. E. (1996), "Etude de la propagation acoustique en espace confiné en présence d'écoulement non isotherme par la méthode des éléments finis", PhD report, Université de Poitiers, Ecole Supérieure d'Ingénieurs de Poitiers, Poitiers, France.

Sadoughifar, A., Farhatnia, F., Izadinia, M., and Talaeetaba, S.B. (2020), "Size-dependent buckling behaviour of FG annular/ circular thick nanoplates with porosities resting on Kerr

foundation based on new hyperbolic shear deformation theory", *Struct*. *Eng*. *Mech*., **73**(3), 225-238. https://doi.org/10.12989/sem.2020.73.3.225.

Safaei, B., Khoda, F.H., and Fattahi, A.M. (2019), "Non-classical plate model for single-layered graphene sheet for axial buckling", *Adv*. *Nano Res*., **7**(4), 265-275. https://doi.org/10.12989/anr.2019.7.4.265.

Selamet A., Radavich PM. (1997), "The acoustic attenuation performance of concentric expansion chambers: an analytical, computational and experimental investigation", *J*. *Sound Vib*., **201**(4),407-426. https://doi.org/10.1006/jsvi.1996.0720.

Shahsavari, D., Karami, B., and Janghorban, M. (2019), "Size-dependent vibration analysis of laminated composite plates", *Adv*. *Nano Res*., **7**(5), 337-349. https://doi.org/10.12989/anr.2019.7.5.337.

Sharma, K.V., Straka, R. and Tavares, F.W. (2020), "Current status of Lattice Boltzmann Methods applied to aerodynamic, aeroacoustic, and thermal flows", *Prog*. *Aerosp*. *Sci*., **115**, 100616. https://doi.org/10.1016/j.paerosci.2020.100616.

Shamshirsaz, M., Sharafi, S., Rahmatian, J., Rahmatian, S., and Sepehry, N. (2020), "A semi-analytical mesh-free method for 3D free vibration analysis of bi-directional FGP circular structures subjected to temperature variation", *Struct*. *Eng*. *Mech*., **73**(4), 407-426. https://doi.org/10.12989/sem.2020.73.4.407.

Tahar, M. and Dias, J.P. (1999), "Propagation et rayonnement acoustique en présence d'un écoulement non uniforme par une méthode de couplage FEM/BEM", *Revue Européenne des Eléments Finis*, **8**, 497-524. https://doi.org/10.1080/12506559.1999.10511395.

Toghraie, D. (2016), "Numerical thermal analysis of water's boiling heat transfer based on a turbulent jet impingement on heated surface", *Physica E*, **84**, 454-465. http://doi.org/10.1016/j.physe.2016.07.017.

Torabi, J., and Ansari, R. (2018), "Thermally induced mechanical analysis of temperature-dependent FG-CNTRC conical shells", *Struct*. *Eng*. *Mech*., **68**(3), 313-323. ttps://doi.org/10.12989/sem.2018.68.3.313.

Tsuji. T., Tsuchiya. T. and Kagawa.Y. (2002), "Finite element and boundary element modelling for the acoustic wave transmission in mean flow medium", *J*. *Sound Vib*., **255**(5), 849-866. https://doi.org/10.1006/jsvi.2001.4189.

Weidong, S.H.A.O. and Jun, L.I. (2019), "Review of lattice Boltzmann method applied to computational aeroacoustics", *Arch*. *Acoust*., **44**(2), 215-238. https://doi.org/10.24425/aoa.2019.128486.

Zhang, J.F., Liu, Q.S., Ge, Y.J. and Zhao, L. (2019), "Studies on the influence factors of wind dynamic responses on hyperbolic cooling tower shells", *Struct*. *Eng*. *Mech*., **72**(5), 541-555. https://doi.org/10.12989/sem.2019.72.5.541.

CC